J Mater Sci: Mater Electron (2022) 33:13657–13667

Early transient creep of single crystal SnAgCu solder joints

Ronit Das[1], Sanoop Thekkut[1], Rajesh Sharma Sivasubramony[1], Thaer Alghoul[1], Atif Mahmood[1], Shantanu Joshi[1], Carlos Arroyo[2], Gaurav Sharma[3], and Peter Borgesen[1,*]

[1] *Department of Systems Science and Industrial Engineering, Binghamton University, Binghamton, NY 13902, USA*
[2] *Texas Instruments, Dallas, TX 75243, USA*
[3] *NXP Semiconductors, Austin, TX 78735, USA*

Received: 23 March 2022
Accepted: 19 April 2022
Published online:
10 May 2022

© The Author(s), under exclusive licence to Springer Science+Business Media, LLC, part of Springer Nature 2022

ABSTRACT

Assessments of solder fatigue life require knowledge of inelastic deformation and damage properties. Previous work showed common constitutive relations for SnAgCu solder joints to be extremely misleading for the kind of joints formed in area array assemblies. At the relatively low stresses in most thermal cycling, room temperature creep rates varied linearly with the stress, rather than with the stress to a power of 4–5 or more as commonly assumed. This is characteristic of creep dominated by diffusion of individual atoms rather than by dislocation motion. The present effort extends this to higher temperatures and the much shorter loading times typical in accelerated thermal cycling testing. It also considers the mobility of dislocations of relevance to recrystallization and damage evolution. The temperature, coarsening of the Ag_3Sn precipitates, and the time of loading all affect the 'cross-over' stress below which inelastic deformation rates are dominated by diffusion. However, the evolution of stresses in cycling is shown to remain totally dominated by diffusion.

1 Introduction

In general, the inelastic deformation of a metal under a load is the sum of the deformation due to dislocation motion and the separate deformation due to diffusion of individual atoms or vacancies. Diffusion creep rates vary linearly with the applied stress whereas dislocation creep rates vary with the stress to a power of 3 (in special cases 2) or more, depending on the rate limiting step. This means that diffusion dominates at low stresses and dislocation motion at higher stresses. One dislocation creep mechanism, so-called Harper–Dorn creep, does also lead to a linear dependence but that mechanism is negligible under practically relevant conditions.

Measurements of the creep of metals have most often been focused on steady-state or 'near-steady-state' creep, for which relatively simple classical models have been established. Emphasis has usually been on dislocation creep which dominates at higher

Address correspondence to E-mail: borgesen@binghamton.edu

https://doi.org/10.1007/s10854-022-08300-y

stresses. The transient creep stage is more complex when it comes to dislocation creep, and most transient dislocation creep models are not physical. A transient diffusion creep model should, however, be simpler.

From the perspective of practical applications, the long-term life of a properly designed microelectronics product is often expected to be limited by the fatigue life of some of the solder joints, motivating massive ongoing testing across the industry. However, interpretation and generalization of accelerated test results require the assumption of a model. Credible modeling of solder joint fatigue is invariably based on the assumption of a damage function and the calculation of stresses and strains vs. time in the cycling involved. The latter requires the assumption of constitutive relations that describe the inelastic deformation properties.

Recent work suggested that the use of common constitutive relations for the kind of SnAgCu joints found in Ball Grid Array (BGA) and Chip Scale Package (CSP) assemblies may be strongly misleading [1, 2]. Indications were that the rate of inelastic deformation at the low stresses of relevance in anything but the most highly accelerated thermal cycling test varies linearly with the applied stress, rather than with the stress to a power of 4 or more as predicted by the constitutive relations. A forthcoming publication will show this to be different for polycrystalline SnAgCu such as that found in die bonds, and so on.

The linear variation suggests that the build-up of stresses in thermal cycling must be dominated by diffusion, rather than by dislocation motion. That does, however, not mean that dislocation motion is unimportant. The final stage in the evolution of damage and failure in a SAC305 joint in thermal cycling is the build-up of dislocation cell structures that coalesce and rotate, eventually leading to recrystallization of the Sn grain and finally crack growth along the evolving high angle grain boundaries [3–5].

Life under long-term use conditions is dominated by the time required for the Ag_3Sn precipitates to coarsen enough so that the recrystallization can begin, whereas life in accelerated thermal cycling is usually dominated by the remaining time for that to lead to failure [5]. Interpretation of test results should account for this difference. The duration of either stage obviously depends on the stresses, and thus on the rates of diffusion, as does the degree of coarsening require for the second stage to begin. However, the latter also depends on the mobility of the dislocations during the high temperature dwell.

A forthcoming publication shows an example of how effects of design and process variations as well as of alloy composition on long-term life may be explained and predicted based solely on measurements of the deformation properties together with the mobility of dislocations.

After briefly summarizing what was learned from our previous results on room temperature creep, the present effort extends this to the higher temperatures dominating the evolution of damage in thermal cycling, to the earlier transient creep of actual relevance, and to the higher stresses where dislocation creep dominates.

2 Background

The stresses on individual solder joints in thermal cycling are usually not experimentally accessible. Stresses have been predicted by Finite Element Modeling, but this was based on constitutive relations derived from measurements of inelastic deformation at stresses where dislocation creep dominates. A 'deconstructed thermal cycling' experiment did, however, allow the direct measurement of applied loads on the joints in a specially designed test vehicle. An average shear stress of 10 MPa at a maximum temperature of 100 °C led to the start of recrystallization in typical BGA joints right away and the joints failed after about 60 cycles [5]. Stresses are certain to be much lower than this in regular thermal cycling and, in particular, long-term service.

Well-established models exist to help identify the dominant creep mechanisms and generalize measured rates of steady-state creep [6]. Fewer models have been proposed for transient creep, but in general the rate of inelastic deformation is still the sum of effects of dislocation motion and the separate diffusion of individual atoms or vacancies. The simplicity of the diffusion creep phenomenon also allows us to argue that transient diffusion creep rates must vary linearly with the stress as well. Dislocation creep rates involve a sequence of steps, including climb over precipitates. In the case of BGA and CSP type joints, measured dislocation creep rates vary with the stress to a power of 4–5 or more [7–12]. Diffusion must therefore dominate at sufficiently low stresses.

The critical requirements for a linear dependence are that the moving species do not interact and that their transport is not affected by stress-dependent changes to the medium (solder). One dislocation creep mechanism, so-called Harper–Dorn creep, also leads to a linear dependence but that mechanism is negligible except at such high temperatures and exceedingly low stresses that nucleation and multiplication of dislocations is insignificant [13–16]. Observation of a linear dependence, whether for steady state or for transient creep, under relevant conditions is therefore a safe indication that the overall creep is dominated by diffusion [1, 3, 17].

We have shown the establishment of steady-state creep in SnAgCu to take longer, probably much longer, than 24 h [2]. This is, of course, much too long to be relevant to thermal cycling. Because of this, and for reasons of practicality, our previous work reported creep rates after 3 h at a constant load. The 'late transient' creep rates of BGA joints measured at that stage were seen to vary linearly up to a uniaxial stress of about 22 MPa. As mentioned, this is high enough to cover stresses of relevance in long-term service and most accelerated thermal cycling tests [5]. In addition, we have shown the room temperature creep rates to vary with the evolution of dislocation structures in thermal cycling [3], consistent with an additional contribution from diffusion along the network of dislocation cores.

The rates of inelastic deformation of an alloy like Sn3Ag0.5Cu (SAC305) depend on the Sn grain morphology and density of the Ag_3Sn precipitates [3, 18, 19]. Each BGA and CSP type joint is formed in a single solidification event during cool-down from reflow, leading to a single crystal or cyclically twinned ('beach ball') structure with no conventional grain boundaries [1, 4, 20, 21]. The present work is limited to this kind of structure. The solidification temperature varies systematically with the joint volume, pad sizes, and pad finishes, leading to strong variations in the precipitate distributions [20, 22, 23]. It is therefore important to measure the properties of realistic joints, rather than macroscopic dog-bone samples. Impression creep measurements are particularly suited for this, averaging over areas encompassing enough Ag_3Sn precipitates to minimize statistical variations of these while still allowing for multiple measurements on one joint.

3 Experiments

Some of the deformation properties of the extremely anisotropic Sn crystals vary significantly with crystal orientation, making it important to limit our creep measurement to single grains. Unlike indentation creep, impression creep allows us to reach steady state at a constant load. That does, however, take too long to be practical for SnAgCu solders and the present work is focused on early transients. Nevertheless, impression creep also has the advantage of averaging over a significant number of precipitates while still limiting our measurements to a particular orientation [2, 24].

Individual Sn3Ag0.5Cu solder spheres of 30 mil diameter were reflowed onto 22 mil diameter Cu pads on printed circuit boards (PCBs) with 1.27 mm pitch. This process was carried out in an N_2 environment in a 10-zone full convection oven with less than 50 ppm oxygen. The peak reflow temperature was 245 °C with about 60 s above liquidus and the average rate of cool-down until solidification was about 2 °C s^{-1}. To ensure that a series of measurements were all done on the same Sn grain the samples were carefully cross-sectioned approximately halfway through the joints and then polished till 0.25 µm of diamond solution followed by colloidal silica solutions of 0.02 µm. These joints were then inspected by cross-polarizer microscopy.

Creep was measured in an Instron Micro-Mechanical Tester using a 10 N load cell with a displacement resolution of 30 nm. The impression creep approach was described by Dutta et al. [25, 26] and Li [24] justified the same. All the measurements were performed using a cylindrical tungsten carbide punch of 100 µm in diameter. The solder surface was first forced to conform to the punch surface by briefly preloading the samples to reach a depth of about 15 µm. Following this, the samples were allowed to relax long enough to complete any inelastic deformation and then the load was raised quickly to the level of actual interest. The loading ramp was kept to less than 4 s. The impression depths were finally measured as a function of time while maintaining a fixed load to keep the elastic deformation of solder and machine constant.

As described by Hyde et al. [27] impression depths were converted to strain by dividing with the diameter of the punch and then multiplying with a correction factor of 0.755. This provides a quantitative

conversion to uniaxial strain in steady state but is only used for comparisons here. The load applied by the punch was converted to a corresponding uniaxial stress by dividing it with the area of the punch and then multiplying with a correction factor of 0.296 [26].

For studies of effects of thermal aging, cross-sectioned samples were polished at least to an additional 20 μm after every stage of aging to eliminate the effects of surface diffusion on precipitate coarsening.

M1m optical and scanning electron microscope (SEM) were used for inspecting the microstructure of the solder joints.

4 Results and discussion

Figure 1 shows a typical example of the variation of the transient creep rate of a SAC305 joint after 15 min of loading with the applied stress. Like in steady state, diffusion creep dominates at low stresses, leading to a linear variation there, while dislocation creep leads to a faster variation at higher stresses. The cross-over between the two regimes is seen to occur at a higher stress than reported after 3 h of loading [2]. On the other hand, as we shall see, the activation energy for dislocation creep is considerably higher so the cross-over is reduced at higher temperatures and of course after coarsening of the precipitates.

As mentioned above, impression measurements require preloading to first mate the punch to the solder surface. Dutta et al. [25, 26] and Li [24] allowed the sample to relax at a negligible load for a while

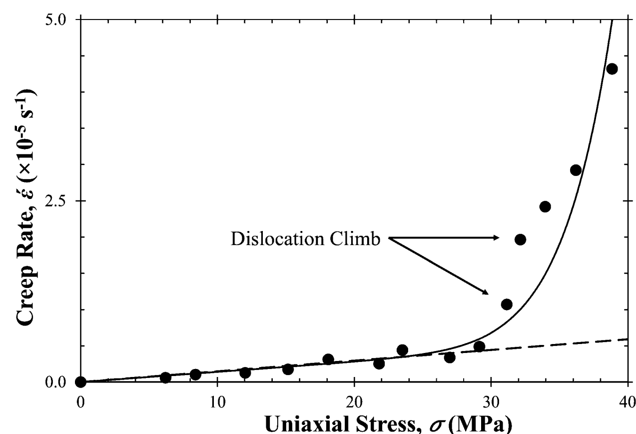

Fig. 1 Early transient creep rates of Sn3Ag0.5Cu joints measured after 15 min. Broken line represents the linear dependence at low stresses and the solid curve represents a fit to a sum of that and a power dependence

after that before performing the actual creep experiment. We conducted first a set of experiments to assess the relaxation time required in our experiments.

4.1 Preload

The Sn crystal structure is, as said, highly anisotropic and some properties may vary strongly from joint to joint. However, we have previously shown the diffusion creep rate after, say, 3 h of loading to not vary by much [2]. We tentatively ascribed this to atoms diffusing away from the point of loading and then toward the open surface in all directions perpendicular to the load.

Much earlier diffusion creep rates also did not vary strongly from joint to joint. At the stresses of interest, typical strains are too small to resolve the variation with time over the first few seconds very well. In the following, we therefore report the average creep rate over the first 30 s. To begin with, 12 different joints were each subjected to a stress of 18.4 MPa, leading to creep dominated by diffusion.

Figure 2a shows average diffusion creep rates for 4 different joints, each after preloading followed by 60 min of relaxation before measuring. The rates are not significantly different from joint to joint. Figure 2b shows the same for relaxation times of 40 min and 20 min as well. Statistical testing showed no significant effect of the relaxation time (p value of 0.972) across this range.

Another experiment showed no significant difference ($p = 0.86$) between creep rates at a stress of 21.7 MPa after relaxation times of 10 min and 20 min (Fig. 3a). However, if the sample was only allowed to relax for 5 min after the preload, subsequent diffusion creep rates were significantly higher ($p = 0.016$).

Dislocation creep rates, on the other hand, did not vary with relaxation times across the same range. Figure 3b shows creep rates for 18 different joints each measured as averages over the first 30 s at a stress of 35 MPa. As we shall see below, this stress should be high enough for dislocation creep to dominate. There is no significant effect of relaxation times of 5 min or more ($p = 0.88$).

The observation of higher diffusion creep rates after preloading is consistent with the assumption that most of the diffusion occurs along the network of dislocations piled up against the Ag_3Sn precipitates during preloading. Incidentally, this also explains

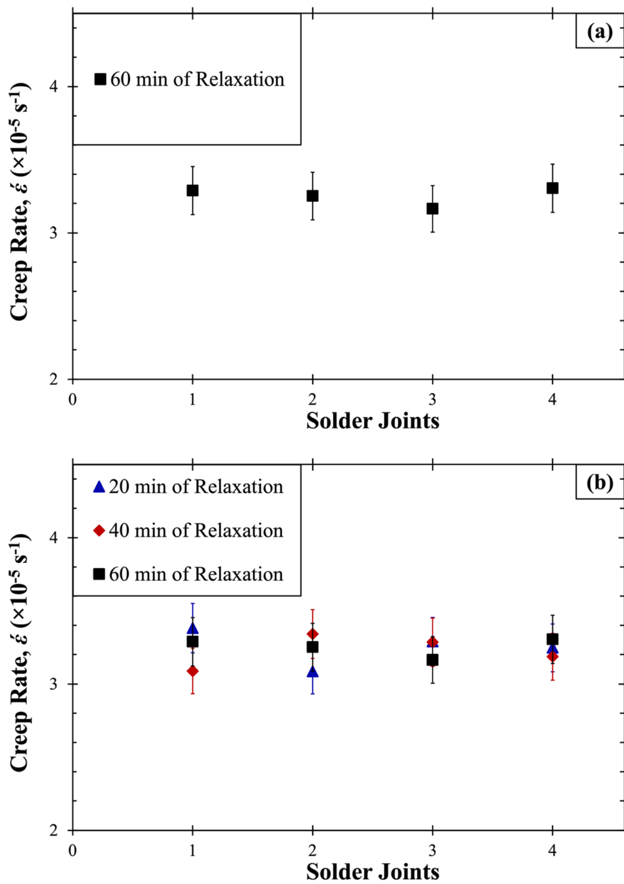

Fig. 2 **a** Average diffusion creep rate over the first 30 s measured on different joints at a load of 18.4 MPa after a brief preload followed by 60 min of relaxation and **b** similar measurements after 40 min and 20 min of relaxation

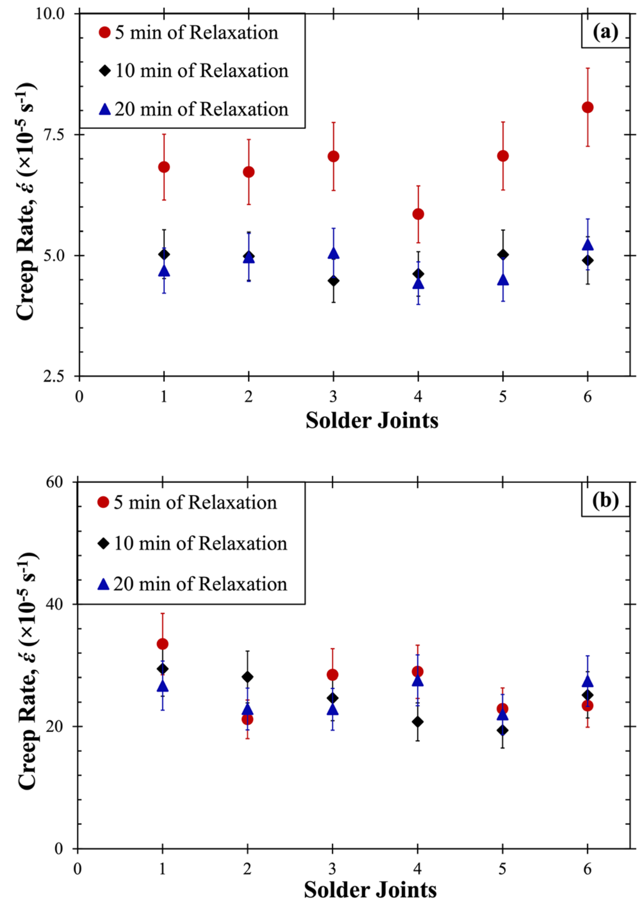

Fig. 3 **a** Average diffusion creep rate over the first 30 s all measured on different joints at a load of 21.7 MPa after a brief preload followed by 5, 10, or 20 min of relaxation and **b** average dislocation creep rate at a load of 35.04 MPa after same relaxation times

why there is no obvious joint to joint variation (effect of Sn grain orientation). The fact that the effect remains more than 5 min after a much shorter preloading then suggests that it takes 5–10 min without a load for the dislocations to redistribute to an even spacing with less interconnected paths.

The remaining experiments all employed relaxation times of 20 min or more after preloading.

4.2 Time dependencies & dominant mechanism

Measurements of the accumulated creep strain necessarily include the strain, ε_o, reached during the initial 3–4 s required to establish a constant load. The century-old Andrade's law [28, 29] predicts an accumulated dislocation creep strain that starts out varying with the time to a power of 1/3 or more. This is ascribed [30] to the ongoing piling up of more dislocations (work hardening) so there is no reason to expect the same to apply for diffusion creep. However, our data are very well matched by a power dependence, at least over the first 15 min.

$$\varepsilon = \varepsilon_o + a * t^n \tag{1}$$

The creep rates in Fig. 3a were all extracted from measurements in which the load was actually maintained up to 15 min. Figure 4a shows one of the curves obtained with a 20 min relaxation time after the preloading. This is seen to be fitted well with a power $n = 0.41$. In fact, all curves obtained after 10–20 min of relaxation led to n values between 0.38 and 0.42. Not surprisingly, the power increases after longer times, reaching 0.5 after 3 h [2].

Anyway, all the dislocation creep curves from which the average rates, in Fig. 3b, were extracted led

to n values between 0.49 and 0.53 for times up to 15 min. In fact, all those curves could be fit with a power of $n = 0.52$ between 0.5 and 900 s. Figure 4b shows an example of such a fit.

The faster increase of the dislocation creep strains with time explains why the cross-over stress above which the dislocation creep rates dominate is lower after longer times of loading.

A series of measurements were conducted of the accumulated creep strain up to 15 min at a given stress. Figure 5a shows the creep rate after a min to vary linearly up to a stress of 31.15 MPa and cross-over to a faster variation with stress above that. A log–log plot (Fig. 5b) points to a power $n = 5.2$ up to 51 MPa, suggesting climb-controlled dislocation creep [31].

However, the cross-over happens at a slightly lower stress of 29.1 MPa for creep rates measured after 15 min at each load (Fig. 1). The corresponding log–log plot (Fig. 6) here suggests a power of $n = 5.35$ from there up to 51 MPa [31], i.e., the same as after 1 min. The cross-over drops further after longer loading, dislocation creep dominating at stresses above 20 MPa after 3 h [2].

Measurements of the temperature dependence of the creep are complicated by the simultaneous effects of precipitate coarsening at higher temperatures.

4.3 Effect of annealing

Figure 7 shows the effect of different lengths of annealing at 125 °C on the room temperature creep rate after 15 min at a stress of 35 MPa. Each point in this plot is an average of measurements on 6–8 different spots. The dislocation creep rate is seen to increase rapidly over the first 100 h of annealing, after which it starts to level off. This is consistent with previous assessments of the effect of aging on the

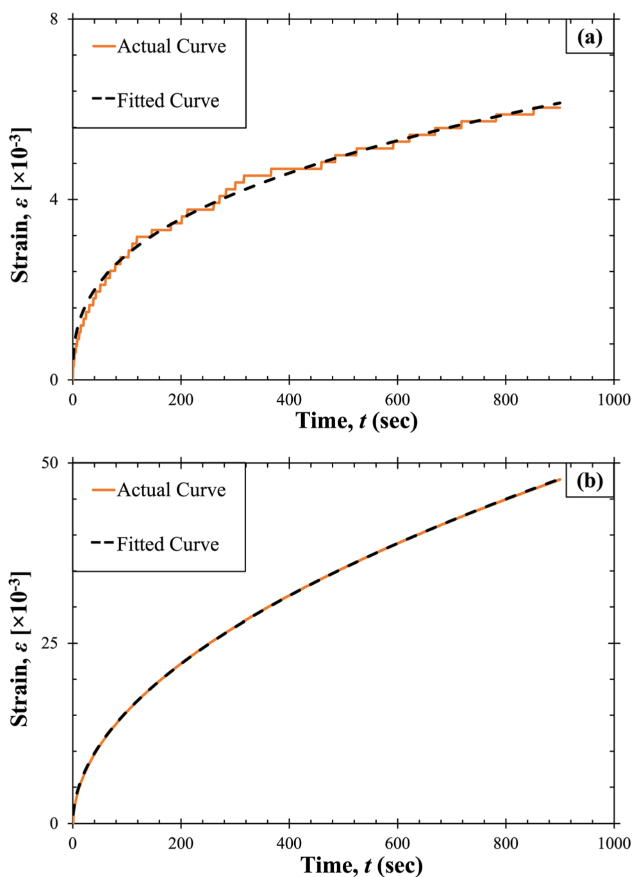

Fig. 4 Creep strain vs. time for Sn3Ag0.5Cu up to 15 min under a constant stress. **a** Diffusion creep at 21.58 MPa. Broken curve: $\varepsilon_o + a^*t^{0.41}$—dependence and **b** Dislocation creep at 35.12 MPa. Broken curve: $\varepsilon_o + a^*t^{0.52}$—dependence

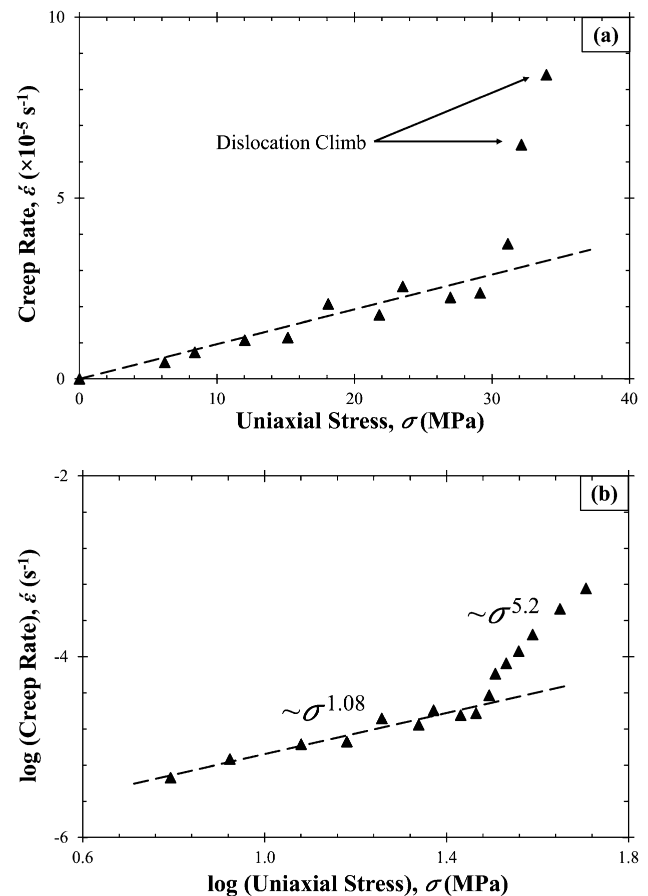

Fig. 5 **a** Early transient creep rates of Sn3Ag0.5Cu joints measured after 1 min at load at room temperature and **b** log–log plot of the creep rates with a straight-line fit corresponding to $n = 1.08$

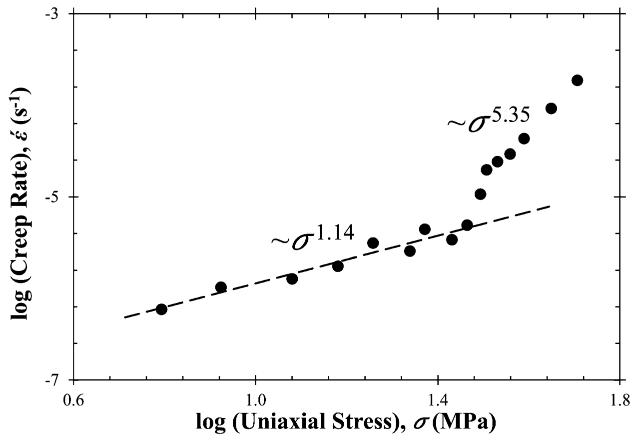

Fig. 6 Log–log plot of creep rates vs. stress after 15 min from Fig. 1 with a straight-line fit corresponding to n = 1.14

hardness [32] and shear strength of Sn3Ag0.5Cu solder joints [33].

Figure 8b shows the stress dependence of the dislocation creep rate to not be significantly different after annealing for 100 h at 125 °C, i.e., the rate limiting step appears to still be dislocation climb over the coarsened precipitates. For some reasons, the diffusion creep rates are also enhanced by annealing (Fig. 8a), presumably reflecting a larger density of interconnected diffusion paths along the dislocation network. However, this enhancement is not as strong, so the cross-over between the diffusion and dislocation creep-controlled regimes is reduced from 29.1 to 17.5 MPa.

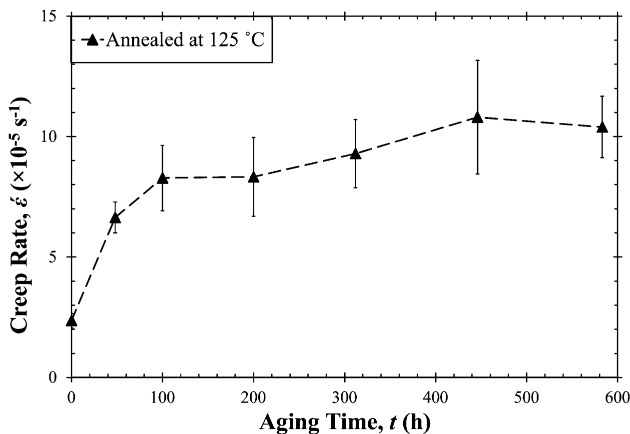

Fig. 7 Room temperature dislocation creep rates of SAC305 solder joints after 15 min at a stress of 35 MPa vs. preceding annealing time at 125 °C. Each data point represent the average of 6–8 measurements

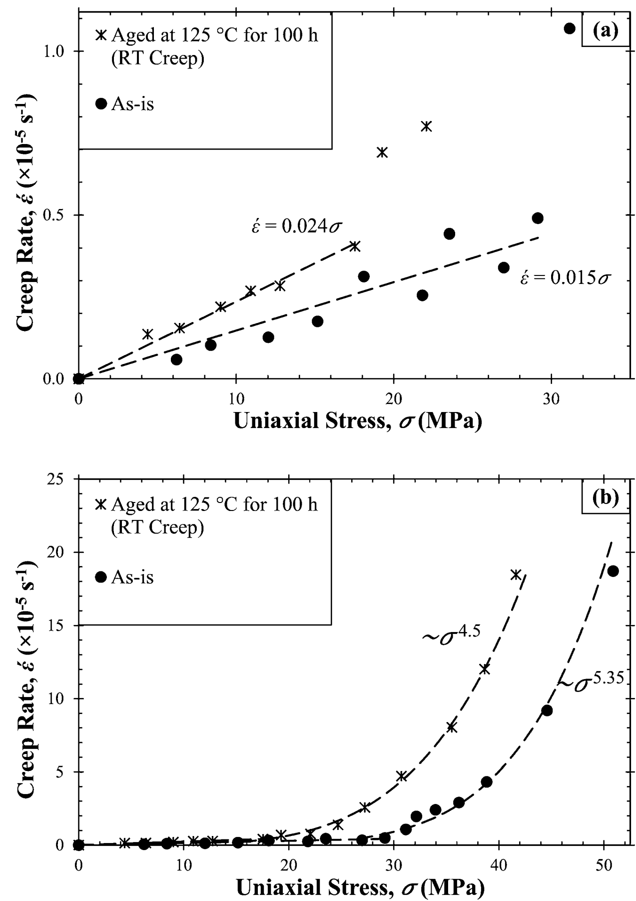

Fig. 8 Room temperature creep rates after 15 min at fixed load for as-is SAC305 and after annealing at 125 °C for 100 h. **a** Diffusion creep regime, and **b** dislocation creep regime

4.4 Effect of temperature

Previous assessments of the effect of temperature were complicated by coarsening of the Ag_3Sn precipitates during the measurements at elevated temperatures [3]. Samples were therefore first annealed for 100 h at 125 °C to stabilize them. Figure 9a shows the variation of the diffusion creep rate with temperature up to 100 °C. Figure 9b shows an Arrhenius plot of the slopes in Fig. 9a. The straight-line fit has a R^2 value of 0.99 and points to an activation energy of 0.21 eV. This would seem to be consistent with rapid diffusion on the loading induced network of dislocations as also suggested by the effect of preloading above.

Li and Basaran [34] argued that the effective diffusivity of undamaged SnAgCu is dominated by the high mobility of the Cu in the lattice and suggested an activation energy for lattice diffusion of only

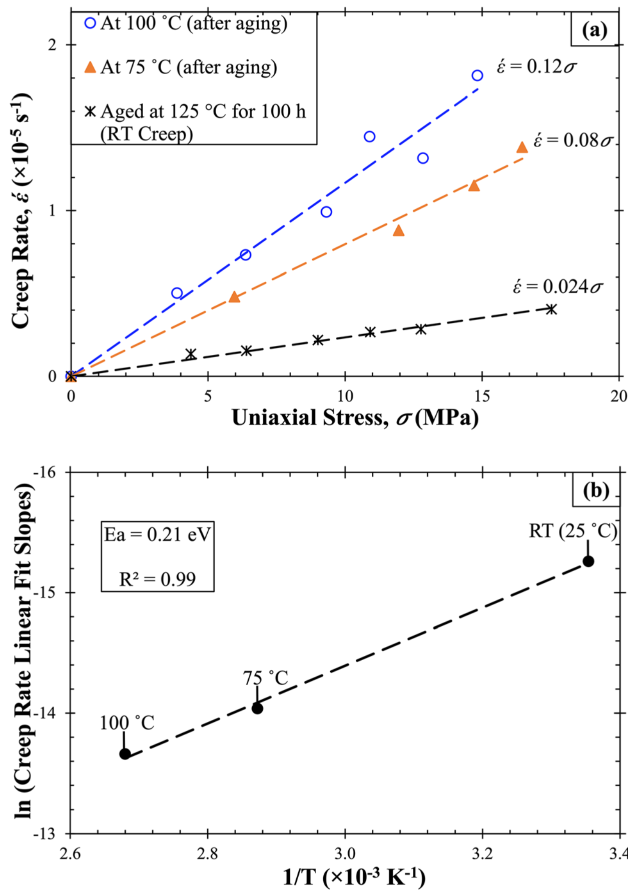

Fig. 9 **a** Diffusion creep rates after 15 min at fixed load for pre-annealed SAC305 at room temperature, 75 °C and 100 °C and **b** Natural logarithm of the linear fit slopes vs. the inverse of the absolute temperature. Straight line reflects an activation energy of 0.21 eV

0.35 eV, much lower than the activation energy for lattice diffusion of Sn through pure Sn [35, 36]. It remains to be determined whether diffusion of the Cu also dominates transport along the dislocation network. Sellers et al. [37] extracted activation energies for the self-diffusivity of Sn on different grain boundaries and discussed experimental results from the literature, leading to values ranging from 0.22 to 0.3 eV, depending on the orientation (one grain boundary orientation led to an activation energy of only 0.1 eV, but that was ascribed to 'channels'). We are not aware of values for dislocation core diffusion, but it stands to reason that activation energies would be in the same range.

The activation energy for dislocation creep is higher. Figure 10a shows the creep rates at room temperature, 75 °C, and 100 °C scales so that they overlap in the dislocation creep dominated regime. This required the multiplication of the room temperature and 75 °C creep rates by factors of 33 and 3.45, respectively. This finally leads to the Arrhenius plot in Fig. 10b, according to which the activation energy for dislocation climb should be 0.44 eV.

The higher activation energy explains why the cross-over stress above which dislocation creep starts to dominate was reduced from 17.5 MPa at room temperature to 16.4 MPa at 75 °C and 14.8 MPa at a temperature of 100 °C.

5 Conclusion

The rate of creep of a metal is the sum of independent contributions from dislocation motion and the separate diffusion of individual vacancies. The latter

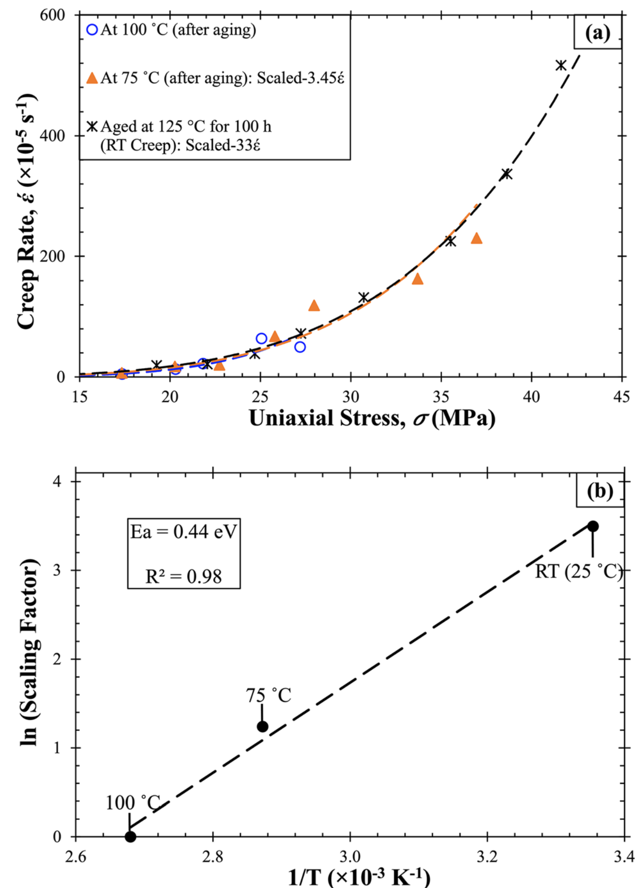

Fig. 10 Dislocation creep rate of pre-annealed SAC305 joints vs. uniaxial stress. **a** Room temperature and 75 °C creep rates have been scaled onto the 100 °C data by multiplying them with a factor of 33 and 3.45. **b** Natural logarithm of their scaling factors vs. the inverse of the absolute temperature. Straight line reflects an activation energy of 0.44 eV

varies linearly with the applied stress whereas the former varies with the stress to a power of 2–3 or more. As a result, a cross-over stress exists below which diffusion creep dominates.

The creep of polycrystalline structures is known to depend on the average grain size. In the case of single crystal or 'beach ball' structure SAC305 joints such as those found in BGA or CSP assemblies, impression creep rates are characteristic of the punch diameter instead.

Early transient diffusion creep rates were found to be enhanced if the sample had been loaded briefly before, whereas dislocation motion appeared to be unaffected.

For any given applied stress, dislocation creep rates vary faster with temperature and slightly faster with time than diffusion creep rates do. Dislocation creep rates are further enhanced by coarsening of the Ag_3Sn precipitates, while separate work has shown them to be reduced by work hardening as one would expect. Overall, the cross-over stress is thus reduced at higher temperatures and after aging induced precipitate coarsening. Coarsening happens faster in cycling, but that also tends to lead to work hardening causing the cross-over stress to increase.

Initial precipitate distributions depend on the combination of solder volumes, pad sizes and finishes, and the rate of cool-down from reflow [38]. The present experimental conditions would here be expected to favor relatively low densities of relatively large precipitates, and thus relatively high dislocation creep rates. One way or the other, even in the absence of work hardening, the stresses near and during the high temperature dwell in thermal cycling are thus going to be dominated by diffusion in any realistic area array SAC305 or SAC405 joints. Early transient creep rates for a particular set of joints may be determined by a single measurement at room temperature together with the assumption of a linear dependence on stress and an activation energy of 0.21 eV.

Acknowledgements

This research was supported by the Semiconductor Research Corporation (SRC) and the State University of New York at Binghamton through the Center for Heterogeneous Integration Research in Packaging (CHIRP, https://www.src.org/program/grc/chirp/), Task No. 2878.012. The authors express their thanks for the discussions and interactions with the SRC Task Liaisons throughout the program.

Authors' contributions

RD contributed to conceptualization, experimentation, literature review, methodology, data curation and figures, validation, investigation, and writing—original draft. ST contributed to experimentation, literature review, methodology, and data curation. RSS contributed to methodology, data curation, and investigation. TA contributed to literature review, investigation, and validation. AM contributed to literature review, validation, and data analysis. SJ contributed to literature review, figure editing, and data analysis. CA contributed to supervision and conceptualization. GS contributed to supervision and conceptualization. PB contributed to supervision, conceptualization, validation, visualization, project administration, funding acquisition, and writing—reviewing & editing. All authors read and approved the manuscript.

Funding

This work was funded by the Semiconductor Research Corporation (SRC) (Funder ID: 10.13039/100000028), and by the State University of New York at Binghamton through the Center for Heterogeneous Integration Research on Packaging (CHIRP) (Grant No. Task 2878.012; Funder ID: 10.13039/100008451).

Data availability

The data and the material generated and/or analyzed during the current study can be reproduced under specified conditions and available upon request.

Declarations

Conflict of interest On behalf of all authors, the corresponding author states that there is no conflict of interest.

Ethical approval The authors state that the work done in the manuscript does not contain any experiment involving human/animal tissue and all the

guidelines were followed according to the journal ethical policy.

References

1. T. Alghoul, D. Watson, N. Adams, S. Khasawneh, F. Batieha, C. Greene, P. Borgesen, Constitutive relations for finite element modeling of SnAgCu in thermal cycling—how wrong we were!, in *Proceedings—Electronic Components and Technology Conference*. (IEEE, Las Vegas, 2016), pp. 1726–1732. https://doi.org/10.1109/ECTC.2016.370
2. T. Alghoul, L. Wentlent, R. Sivasubramony, C. Greene, P. Thompson, P. Borgesen, Diffusion creep of realistic SnAgCu solder joints at times and stresses of relevance to thermal fatigue. IEEE Trans. Comp. Packag. Manuf. Technol. **10**(2), 288–295 (2020). https://doi.org/10.1109/TCPMT.2019.2929051
3. T. Alghoul, L. Wentlent, R. Sivasubramony, C. Greene, P. Thompson, P. Borgesen, Effects of thermal cycling on creep of SnAgCu solder joints. IEEE Trans. Comp. Packag. Manuf. Technol. **9**(5), 888–894 (2019). https://doi.org/10.1109/TCPMT.2018.2884731
4. P. Borgesen, L. Wentlent, T. Alghoul, R. Sivasubramony, M. Yadav, S. Thekkut, J.L.T. Cuevas, C. Greene, A mechanistic model of damage evolution in lead free solder joints under combinations of vibration and thermal cycling with varying amplitudes. Microelectron. Reliab. **95**, 65–73 (2019). https://doi.org/10.1016/j.microrel.2019.02.001
5. P. Borgesen, L. Wentlent, S. Hamasha, S. Khasawneh, S. Shirazi, D. Schmitz, T. Alghoul, C. Greene, L. Yin, A mechanistic thermal fatigue model for SnAgCu solder joints. J. Electron. Mater. **47**(5), 2526–2544 (2018). https://doi.org/10.1007/s11664-018-6121-0
6. T.G. Langdon, Identifiying creep mechanisms at low stresses. Mater. Sci. Eng. A **283**(1–2), 266–273 (2000). https://doi.org/10.1016/s0921-5093(00)00624-9
7. H.G. Song, J.W. Morris, F. Hua, The creep properties of lead-free solder joints. J. Miner. Metals Mater. Soc. **54**(6), 30–32 (2002). https://doi.org/10.1007/BF02701846
8. M. Motalab, Z. Cai, J.C. Suhling, P. Lall, Determination of Anand constants for SAC solders using stress–strain or creep data, in *InterSociety Conference on Thermal and Thermomechanical Phenomena in Electronic Systems, ITHERM*. (IEEE, San Diego, 2012), pp. 910–922. https://doi.org/10.1109/ITHERM.2012.6231522
9. S. Wiese, F. Feustel, E. Meusel, Characterisation of constitutive behaviour of SnAg, SnAgCu and SnPb solder in flip chip joints. Sens. Actuators A **99**(1–2), 188–193 (2002). https://doi.org/10.1016/S0924-4247(01)00880-9
10. M. Pei, J. Qu, Constitutive modeling of lead-free solders, in *Proceedings of the ASME/Pacific Rim Technical Conference and Exhibition on Integration and Packaging of MEMS, NEMS, and Electronic Systems: Advances in Electronic Packaging 2005*. (ASME, San Francisco, 2005), pp. 1307–1311. https://doi.org/10.1115/ipack2005-73411
11. T. Chen, I. Dutta, Effect of Ag and Cu concentrations on the creep behavior of Sn-based solders. J. Electron. Mater. **37**(3), 347–354 (2008). https://doi.org/10.1007/s11664-007-0340-0
12. P. Kumar, Z. Huang, S.C. Chavali, D.K. Chan, I. Dutta, G. Subbarayan, V. Gupta, Microstructurally adaptive model for primary and secondary creep of Sn–Ag-based solders. IEEE Trans. Comp. Packag. Manuf. Technol. **2**(2), 256–265 (2012). https://doi.org/10.1109/TCPMT.2011.2173494
13. J.G. Harper, L.A. Shepard, J.E. Dorn, Creep of aluminum under extremely small stresses. Acta Metall. **6**(7), 509–518 (1958). https://doi.org/10.1016/0001-6160(58)90114-7
14. T.G. Langdon, Creep at low stresses: an evaluation of diffusion creep and Harper–Dorn creep as viable creep mechanisms. Metall. Mater. Trans. A **33**(2), 249–259 (2002). https://doi.org/10.1007/s11661-002-0087-4
15. F.A. Mohamed, Harper–Dorn creep: controversy, requirements, and origin. Mater. Sci. Eng. A **463**(1–2), 177–184 (2007). https://doi.org/10.1016/j.msea.2006.06.142
16. M.E. Kassner, P. Kumar, W. Blum, Harper–Dorn creep. Int. J. Plast **23**(6), 980–1000 (2007). https://doi.org/10.1016/j.ijplas.2006.10.006
17. F. Batieha, S. Hamasha, Y. Jaradat, L. Wentlent, A. Qasaimeh, P. Borgesen, Challenges for the prediction of solder joint life in long term vibration, in *Proceedings—Electronic Components and Technology Conference*. (IEEE, San Diego, 2015), pp. 1553–1559. https://doi.org/10.1109/ECTC.2015.7159804
18. L. Wentlent, T.M. Alghoul, C.M. Greene, P. Borgesen, Effects of amplitude variations on deformation and damage evolution in SnAgCu solder in isothermal cycling. J. Electron. Mater. **47**(5), 2752–2760 (2018). https://doi.org/10.1007/s11664-018-6129-5
19. S. Hamasha, P. Borgesen, Effects of strain rate and amplitude variations on solder joint fatigue life in isothermal cycling. J. Electron. Packag. Trans. ASME (2016). https://doi.org/10.1115/1.4032881
20. D.W. Henderson, J.J. Woods, T.A. Gosselin, J. Bartelo, D.E. King, T.M. Korhonen, M.A. Korhonen, L.P. Lehman, E.J. Cotts, S.K. Kang, P. Lauro, D.Y. Shih, C. Goldsmith, K.J. Puttlitz, The microstructure of Sn in near-eutectic Sn–Ag–Cu alloy solder joints and its role in thermomechanical fatigue. J. Mater. Res. **19**(6), 1608–1612 (2004). https://doi.org/10.1557/JMR.2004.0222
21. L. Yin, L. Wentlent, L. Yang, B. Arfaei, A. Oasaimeh, P. Borgesen, Recrystallization and precipitate coarsening in Pb-

Free solder joints during thermomechanical fatigue. J. Electron. Mater. **41**(2), 241–252 (2012). https://doi.org/10.1007/s11664-011-1762-2
22. T. Bieler, P. Borgesen, Y. Xing, L. P. Lehman, E. J. Cotts, Correlation of Microstructure and Heterogeneous Failure in Pb Free Solder Joints, in *Pb-Free and RoHSCompliant Materials and Processes for Microelectronics*, ed by C.A. Handwerker, K. Suganuma, H.L. Reynolds, J. Bath (MRS Spring Meeting, 2007)
23. L.P. Lehman, Y. Xing, T.R. Bieler, E.J. Cotts, Cyclic twin nucleation in tin-based solder alloys. Acta Mater. **58**(10), 3546–3556 (2010). https://doi.org/10.1016/j.actamat.2010.01.030
24. J.C.M. Li, Impression creep and other localized tests. Mater. Sci. Eng. A **322**(1–2), 23–42 (2002). https://doi.org/10.1016/S0921-5093(01)01116-9
25. I. Dutta, C. Park, S. Choi, Impression creep characterization of rapidly cooled Sn–3.5Ag solders. Mater. Sci. Eng. A **379**(1–2), 401–410 (2004). https://doi.org/10.1016/j.msea.2004.03.023
26. I. Dutta, D. Pan, S. Jadhav, Impression creep testing and microstructurally adaptive creep modeling of lead free solder interconnects, in *Proceedings of the 6th International Conference on Thermal, Mechanical and Multi-Physics Simulation and Experiments in Micro-Electronics and Micro-Systems—EuroSimE 2005*. (IEEE, Berlin, 2005), pp. 641–647. https://doi.org/10.1109/ESIME.2005.1502881
27. T.H. Hyde, K.A. Yehia, A.A. Becker, Interpretation of impression creep data using a reference stress approach. Int. J. Mech. Sci. **35**(6), 451–462 (1993). https://doi.org/10.1016/0020-7403(93)90035-S
28. E.N. Da, C. Andrade, On the viscous flow in metals, and allied phenomena, in *Proceedings of the Royal Society of London. Series A Containing Papers of a Mathematical and Physical Character*. (The Royal Society, London, 1910), pp. 1–12. https://doi.org/10.1098/rspa.1910.0050
29. E.N. Da, C. Andrade, The flow in metals under large constant stresses, in *Proceedings of the Royal Society of London. Series A Containing Papers of a Mathematical and Physical Character*. (The Royal Society, London, 1914), pp. 329–342. https://doi.org/10.1098/rspa.1914.0056
30. F. Louchet, P. Duval, Andrade creep revisited. Int. J. Mater. Res. **100**(10), 1433–1439 (2009). https://doi.org/10.3139/146.110189
31. J. Weertman, Steady-state creep through dislocation climb. J. Appl. Phys. **28**(3), 362–364 (1957). https://doi.org/10.1063/1.1722747
32. V. Venkatadri, *Quantitative Assessment of Long Term Aging Effects on the Mechanical Properties of Lead Free Solder Joints*. (State University of New York at Binghamton, ProQuest Dissertations & Theses Global (305109339), 2009)
33. R. Das, A. Mahmood, S. Thekkut, R. Sivasubramony, M. Njuki, C. Greene, N. Dimitrov, P. Borgesen, *Reliability of Micro-Joints Formed by a Low Temperature Soldering Approach* (Semiconductor Research Corporation—TechCon, Durham, 2021)
34. S. Li, C. Basaran, Effective diffusivity of lead free solder alloys. Comput. Mater. Sci. **47**(1), 71–78 (2009). https://doi.org/10.1016/j.commatsci.2009.06.015
35. J.D. Meakin, E. Klokholm, Self-diffusion in tin single crystals. Trans. Metall. Soc. AIME **218**, 463–466 (1960)
36. C. Coston, N.H. Nachtrieb, Self-diffusion in tin at high pressure. J. Phys. Chem. **68**(8), 2219–2229 (1964). https://doi.org/10.1021/j100790a032
37. M.S. Sellers, A.J. Schultz, C. Basaran, D.A. Kofke, β-Sn grain-boundary structure and self-diffusivity via molecular dynamics simulations. Phys. Rev. B Condens. Matter Mater. Phys. **81**(13), 134111 (2010). https://doi.org/10.1103/PhysRevB.81.134111
38. P. Borgesen, E. Cotts, I. Dutta, Microstructurally adaptive constitutive relations and reliability assessment protocols for lead free solder, in *Proceedings of SMTA International*. (2014), pp. 536–546

Publisher's Note Springer Nature remains neutral with regard to jurisdictional claims in published maps and institutional affiliations.